

Petrophysical Analysis of Reservoirs Rocks at Mchungwa Well in Block 7 Offshore, Tanzania: Geological Implication on the Reservoir Quality

Amina S. Mjili, Gabriel D. Mulibo*

Department of Geology, University of Dar es Salaam, Dar es Salaam, Tanzania

Email: *gmbelwa@yahoo.com

How to cite this paper: Mjili, A.S. and Mulibo, G.D. (2018) Petrophysical Analysis of Reservoirs Rocks at Mchungwa Well in Block 7 Offshore, Tanzania: Geological Implication on the Reservoir Quality. *Open Journal of Geology*, 8, 764-780.
<https://doi.org/10.4236/ojg.2018.88045>

Received: June 5, 2018

Accepted: August 1, 2018

Published: August 3, 2018

Copyright © 2018 by authors and Scientific Research Publishing Inc. This work is licensed under the Creative Commons Attribution International License (CC BY 4.0).

<http://creativecommons.org/licenses/by/4.0/>



Open Access

Abstract

The present work highlights the results of the study conducted to estimate the petrophysical properties of the Mchungwa well with the aim of assessing the quality of reservoirs rocks. A set of well logs data from Mchungwa well were used for the analysis that involved identification of lithology, hydrocarbon and non-hydrocarbon zones and determinations of petrophysical parameters such as shale volume, porosity, permeability, fluid saturation and net pay thickness. This study was able to mark six sandstone zones with their tops and bases. Of the six zones hydrocarbon indication was observed on four zones from which estimation of petrophysical parameters was done to assess the reservoirs quality. The petrophysical parameters across the four reservoirs yield an average shale volume ranging from 0.08 to 0.15 v/v. The porosity ranges from 7% to 23%, indicating a fair to good porosity sandstone, while permeability ranges from 0.01 to 6 mD. The porosity and permeability results suggest that the quality of the sandstone reservoirs identified at Mchungwa well is poor. Fluid types defined in the reservoirs on the basis of neutron-density log signatures and resistivity indicate a mixture of water and gas. However, high water saturation (50% - 100%) indicates that the proportion of void spaces occupied by water is high, thus, indicating low hydrocarbon saturation of 2.4%, 17.9%, 19.2% and 39.3%. Generally the results show that hydrocarbon potentiality at Mchungwa well is extremely low because of small net pay thickness and very low hydrocarbon saturation. This could be attributed to the geology of the surrounding area where low hydrocarbon saturation suggest the presence of non-commercial volumes of either migrant gas or gas generated from the interbedded claystone sediments, which are dominant in the observed well.

Keywords

Offshore, Tanzania, Hydrocarbon, Reservoir, Petrophysical

1. Introduction

Tanzania deep offshore basins are part of the Tanzania coastal basin formed as a result of Gondwana break-up and drifting of Madagascar with respect to the African continental block during the Early Mesozoic time. The exploration Block 7, where Mchungwa well is located, forms part of the deep offshore basins that are known to be petroliferous for hydrocarbon exploration [1] [2]. This is evident by the presence of hydrocarbon shows both at the surface and subsurface in different parts around the surrounding area. The basins occur parallel to the coast and are joined with large, down-to-the-basin faults, which demarcate the present coastline (Figure 1).

The basins are mainly composed of thick Mesozoic and Tertiary successions with approximately 4000 m thickness, which overlap the continent-ocean boundary [3] [4] [5]. Several Mesozoic-Tertiary potential marine organic-rich source

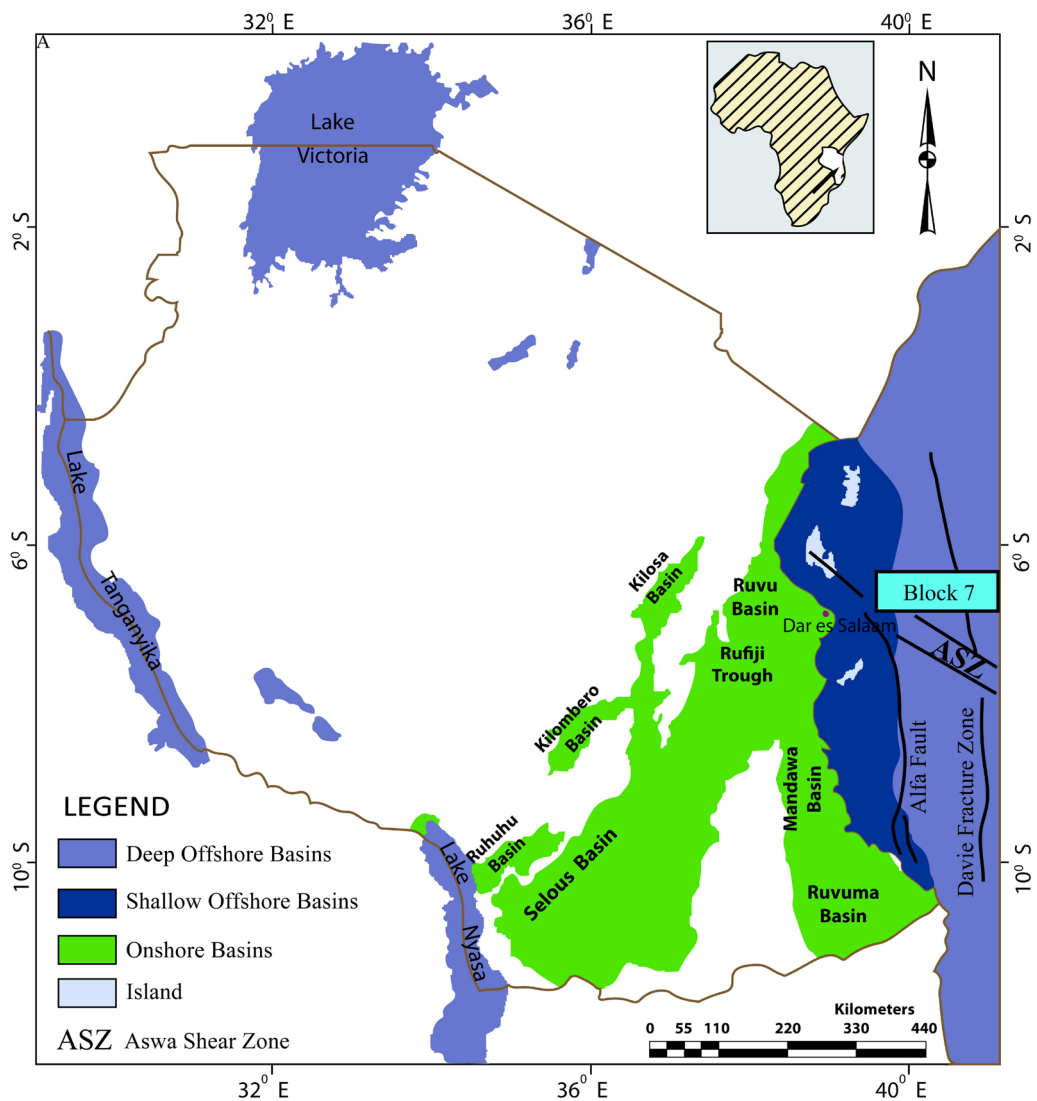


Figure 1. Map showing the Tanzania sedimentary basins including offshore basins (modified after [12]).

rocks are present and four regional potential source intervals have been recognized [2] [6]. These include Cretaceous sandstone, a regional proven reservoir, and Tertiary deltaic sandstones and limestone are local proven reservoirs. Cretaceous siltstones and shale are regional seals and Jurassic evaporates provide local effective seals.

Despite the presence of hydrocarbon discoveries in various parts along the Tanzania offshore basins, little is documented about petrophysical properties of reservoir rocks at the Mchungwa well in Block 7. A total of 57 TCF has recently been discovered in Cretaceous and Tertiary sandstone reservoirs in the nearby exploration Blocks 1 - 4 in southern part (TPDC 2015-unpublished report). Despite its similarities in lithology and age of reservoir with other discovered reservoirs, reservoir units and their borehole thicknesses of Mchungwa well in Block 7, which indicate potential for petroleum system, are not well established. During drilling, gas mud and fluoresces were observed, indicating the presence of hydrocarbons the scenario that leaves a question as to which reservoir interval(s) contain hydrocarbons and at what proportion (Ophir Dominion Ltd, 2014-unpublished report). Identification of reservoir units and their thickness paves the way in understanding the reservoir rocks and their characteristics. This study therefore uses well log data to study the petrophysical characteristics of the reservoir rocks at Mchungwa well in Block 7 in order to assess the quality of the reservoirs encountered in the well. Results from this study advance our understanding on the relationship between the petrophysical properties and hydrocarbon system of the offshore Block 7 and in other nearby blocks. Moreover, the petrophysical information obtained from Mchungwa well provides vital information on the quality of reservoirs and also a source of information to further exploration in relation to the geological processes.

2. Geology and Tectonic Setting

2.1. Regional Geology and Tectonic Setting

Development of Tanzania coastal and offshore basins was the result of the progressive break-up of Gondwana. Initial rifting and drift of the margin began with the Karoo system of the Permo-Triassic with fluvial continental floodplain, deltaic and lacustrine deposits including occasional marine incursions. Karoo rifting proceeded and activated the extensional tectonics, which resulted in the formation of two intracratonic NE-SW, and NW-SE Permo-Triassic faults named as Tanga and Lindi faults respectively (**Figure 1**) [1]. Prior to the occurrence of rifting, two old lineaments, the WNW-ESE Utete-Tagalala and the NW-SE Aswa were already formed which together with other faults controlled the distribution and deposition of Karoo sediments in varying environments [7] [8] [9].

The drift phase began in the Middle Jurassic, the period in which East and West Gondwana separated and East Gondwana broke up into the continental plates of India, Antarctica, and Australia. This period was associated with wide-

spread igneous activities and opening of the Somali basin as Madagascar moved from the East African coast to its present position [3] [9] [10]. The ESE movement of Madagascar was controlled by a north-south trending transform fault, the Davie ridge [3] [4] [9]. The continental margins of the fragmented continents underwent gradual thermal subsidence during the Bajocian where by restricted marine syn-rift sediments were deposited into the basin, flooding the intra-continental Karoo sequence. The accumulation and preservation of marine organic matter into this restricted marine basin forms the primary source rocks for the margin [9]. The final phase of the Gondwana breakup is characterized by the termination of tectonic activity and the formation of passive margins of the Somali Basin [9].

Regional structural trends of Tanzania coastal and offshore basins follow the Tanga and Lindi Permo-Triassic faults, which strike in the NNE-SSW and NNW-SSE respectively, with some young onshore faults oriented along the same trends. The offshore structures are post Karoo faults whose trends have been rejuvenated from older ones. The orientation of structural features runs parallel to the present coastline [9] [11].

2.2. Local Geological Setting

Block 7 is located offshore northern Tanzania, connecting the southern portion of the Pemba-Zanzibar sub-basin and the northern section of the Mafia Deep sub-basin, which is part of the Tanzania coastal basins (Figure 1). The Mchungwa well within Block 7 confirms the Tertiary and Cretaceous stratigraphy present in Block 7 and the sequence stratigraphic correlation from the southern Tanzania offshore wells (Ophir, Dominion Tanzania Ltd, 2014-unpublished report). In Block 7 there are three prominent tectonic elements [12] (Figure 1). The first tectonic element is the Davie Fracture Zone (DFZ), representing the right-lateral wrenching of Madagascar away from the African coast. West of this zone, synrift sediments of Triassic to Early Jurassic age are overlain by post Middle Jurassic to Recent post rift sequences [13].

The second one is the Aswa Shear Zone, which is a reactivated Precambrian NW-SE oriented feature extending onshore. The last tectonic element in Block 7 is the Sea Gap Fault, which is visible in the Cretaceous sequence but does not extend into the Tertiary. The youngest sediments examined at Mchungwa well were claystone, aged Upper to Middle Eocene while the deepest age-assigned in claystone rock is considered to be Valanginian to Tithonian in age. Dominant lithologies at Mchungwa well include claystone, siltstone, sandstone and limestone.

3. Material and Methods

Digital well logs from Mchungwa well obtained from Tanzania Petroleum Development Company (TPDC) were used for this study to analyze the petrophysical properties of the reservoir rocks. The qualitative and quantitative evaluation

of these properties was inferred from wireline logs, which include caliper, gamma ray, resistivity, sonic, neutron and density logs. The analysis of petrophysical properties from well logs each of which is described in the following section was done using Techlog software version 2013.4.0.1.

3.1. Lithological Identification from Gama Ray (GR) Log

The gamma ray (GR) log measures the natural radioactivity of the formation in the borehole versus depth. The lithological identification was done by reading API values on the gamma ray curve. In the curve the shale free lithology like sandstone and carbonate show low gamma ray values (≤ 60 API) whereby shale (black shale and marine shale) exhibit relatively high GR count rates (≥ 60 API) (Figure 2) due to presence of potassium ions in their lattice structure [14].

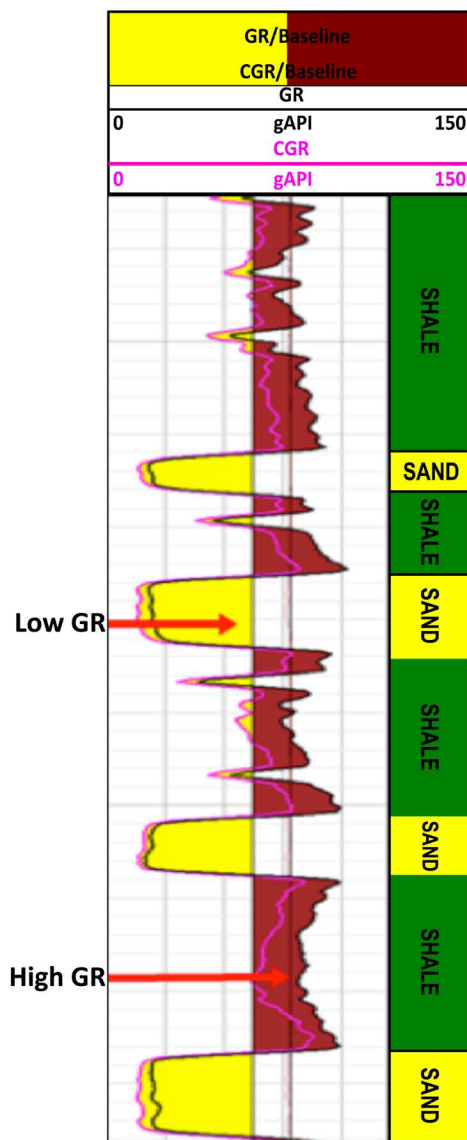


Figure 2. Gamma ray (GR) log plot showing API Unit ranging from a low value of zero to as high as 150 API.

3.2. Lithological Identification from Photoelectric Factor (PEF)

The PEF log is sensitive to differences in the mean atomic number of the formation and it is insensitive to the porosity and fluid saturation of that lithology, which makes the PEF log a good indicator of lithology. The response of the tool to common rock types used in lithology identification is given in **Table 1** [15].

3.3. Lithological Identification from Neutron-Density Logs

A combination of neutron and density logs were sketched together in the same track, and low values on both logs represents sandstone formation, overlap of the two log curves indicates limestone lithology and high values on both logs indicate shale lithology. In addition to using neutron-density logs separation for differentiating two lithology, in this study the logs were also used to create a neutron-density cross plot. The cross plots were obtained by plotting together neutron and density logs where sandstone, carbonate and shale lithology were displayed. Observing points falling within a lithology region and using gamma ray log scale, rock types were identified.

3.4. Reservoir Identification

Reservoir rocks, which are porous and permeable sedimentary rocks containing water, oil or gas in their pore spaces, were identified using the gamma and the porosity (neutron-density) logs. Common reservoir rocks are sandstones and carbonate. Sandstone reservoirs exhibit very low radioactivity, because of low concentrations of radioactive elements [16] [17]. Porosity tools are also important in locating reservoir zones in a sense that each porosity tool should give a reading in porous zones which, when converted to porosity as a function of lithology, will show the same porosity in reservoirs free of gas and clay effects [17].

3.5. Fluid Type Identification

Reservoirs may contain water, hydrocarbons or both and in this context it is therefore important to identify which type of fluid is contained in the reservoir. Resistivity logs were used to distinguish between water bearing zones, and hydrocarbon bearing zones while porosity logs were used in identifying hydrocarbon interval especially gas bearing interval.

In hydrocarbon bearing formations, the resistivity log signatures show higher resistivity values than in water bearing formations. In gas zones, neutron log records lower hydrogen content, thus a higher count rate resulting in low porosity

Table 1. Relative gamma ray values for common sedimentary rocks.

Lithology	Clean sandstone	Shale	Dolomite	Limestone	Dirty sanadstone
PEF value in barns/electron	1.7 - 1.8	3.5 - 4.0	3	5	15 - 150

while density log in gas zone reduces bulk density, resulting in a high apparent porosity. This effect causes the occurrence of crossover between neutron and density logs. The presence of crossover in the logs is an indicator of hydrocarbon and this study was able to identify the crossovers at different depth intervals.

3.6. Shale Volume Estimation

The shale volume was calculated using the Larionov [18] model (Equation (1)) among other non-linear models for older rocks because reservoir rocks at Mchungwa well are of Cretaceous age.

$$V_{SHLarionov}(1969) = 0.33 * (2^{(2 * I_{GR})} - 1) \quad (1)$$

where V_{SH} is the shale volume and I_{GR} is the gamma ray index which was obtained using Equation (2).

$$I_{GR} = \frac{GR_{log} - GR_{min}}{GR_{max} - GR_{min}} \quad (2)$$

where I_{GR} is gamma ray index, GR_{log} is the gamma-ray reading for each zone, GR_{min} and GR_{max} are the minimum and maximum gamma-ray values for clean sand and shale respectively.

3.7. Porosity Determination

In this study total and effective porosities of the selected reservoirs zones were calculated using density logs. These parameters are determined by substituting the bulk density readings obtained from the formation density log within each reservoir into Equation (3). In the equation, the formation bulk density (ρ_b) is related to formation matrix density (ρ_{ma}) and formation fluid density (ρ_f) as follows.

$$\phi = \frac{\rho_{ma} - \rho_b}{\rho_{ma} - \rho_f} \quad (3)$$

where ϕ is total porosity, ρ_{ma} is matrix (or grain) density for sandstone, ρ_b is bulk density from log, ρ_f is fluid density.

3.8. Water Saturation Determination

Determination of water saturation is the key parameter from which initial hydrocarbon in place can be estimated during formation evaluation. In this study, the Archie's and Indonesia's models were used to calculate water saturation depending on whether the reservoir is clean sand or shaly sand and their results were compared.

3.8.1. Archie Equation Model

This is the common model that is used to calculate water saturation in clean lithology (*i.e.*, clean sand or carbonate). Archie's equation used for determination of water saturation is given in Equation (4) as [19]:

$$S_w = \sqrt[n]{\frac{a * R_w}{\phi^m * R_t}} \quad (4)$$

where R_w is the water resistivity at formation temperature, R_t is the true resistivity, $\frac{a}{\phi^m}$ is the formation factor (F) in which “a” represents constant related to texture, (assumed to be approximately 1 for sandstone), “ ϕ ” is the porosity, “m” is the cementation exponent and “n” is the saturation exponent.

3.8.2. Indonesian Model

Indonesian model introduced by Poupon and Leuveaux [20] is used to calculate the water saturation in shaly sand reservoirs. The main inputs are the effective porosity (ϕ_e), shale volume (V_{sh}), shale resistivity (R_{sh}), water resistivity (R_w) and deep resistivity (R_t). It is given in Equation (5) below.

$$S_w = \left\{ \left[\left(\frac{V_{sh}^{2-V_{sh}}}{R_{sh}} \right)^{\frac{1}{2}} + \left(\frac{\phi_e^m}{R_w} \right)^{\frac{1}{2}} \right]^2 R_t \right\}^{-\frac{1}{n}} \quad (5)$$

3.9. Net Pay

A porosity cut-off of 10% as minimum value and 25% as a maximum value, along with a shale volume cut-off of 0% as minimum value and 25% as maximum value were used to define the quality of the reservoir rock. Water saturation cut-off value of 50% was used to define pay zone. The reservoirs were defined by the porosity greater than 10% and shale volume less than or equal to 25%. For the net pay, if the water saturation within the reservoir is less than 50%, the reservoir is considered to contain hydrocarbon.

3.10. Hydrocarbon Saturation (S_h)

This is the amount or percentage of hydrocarbon that occupies the pore space computed by subtracting the percentage of water occupying the pore space (water saturation) from 100% as indicated in Equation (6) below.

$$S_h = (100 - S_w) \% \quad (6)$$

3.11. Permeability Estimation

The permeability of each delineated reservoir at Mchungwa well was estimated using equation below [21].

$$K = 0.136 \frac{\phi^{4.4}}{S_{wir}^2} \quad (7)$$

where K is the permeability in mD, ϕ is Effective porosity in v/v and S_{wir} is the irreducible water saturation in v/v. In this study the permeability was estimated first by using the calculated water saturation, and then the results were compared with those estimated from Crain’s method [22] using irreducible wa-

ter saturation, S_{wirr} from Crain's method is given by Equation (8) below.

$$S_{wirr} = \frac{\phi \times S_w}{\phi_{eff}} \quad (8)$$

where ϕ_{eff} = effective porosity and $\phi \times S_w$ is the Bulk Volume Water (BVW).

A reservoir at irreducible water saturation exhibits BVW values that are constant throughout but if the BVW is not constant means that the reservoir or zone is not at irreducible water saturation [16].

4. Results

4.1. Qualitative Results

4.1.1. Lithology Results

Three main lithologies are identified at Mchungwa well, which include shale, sandstone and little carbonate from lithology identification logs (gamma, neutron-density combination, cross plot and photoelectric factor (PEF)). Six (6) clean sand formations marked as zones A, B, C, D, E and F with their depth range have been identified and presented in **Figures 3-8** and **Table 2**.

4.1.2. Hydrocarbon and Non-Hydrocarbon Bearing Zones

Hydrocarbon zones were identified qualitatively by using neutron-density logs combination and resistivity logs. Based on visual observation from these logs, four zones marked by C, D, E and F among six selected reservoir zones were identified as gas bearing zones. These zones were identified depending on the presence of neutron-density crossovers and high resistivity values in these zones,

Table 2. The type of lithology identified from gamma ray log, neutron-density combination and PEF.

Depth	Lithology	Remark
3189.4 - 3233.0	Sand	
3233.0 - 3250.0	Shale	Zone A
3255.2 - 3346.1	Sand	
3346.2 - 3383.3	Shale	Zone B
3383.9 - 3605.9	Sand	
3607.1 - 3682.9	Shale	Zone C
3683.1 - 3911.8	Sand	
3912.0 - 4687.0	Shale	Zone D
4688.1 - 4701.0	Sand	
4701.0 - 5044.9	Shale	Zone E
5044.9 - 5118.1	Sand	
5118.1 - 5304.0	Shale	Zone F
5305.0 - 5477.6	Sand	
5477.6 - 5775.0	Shale	

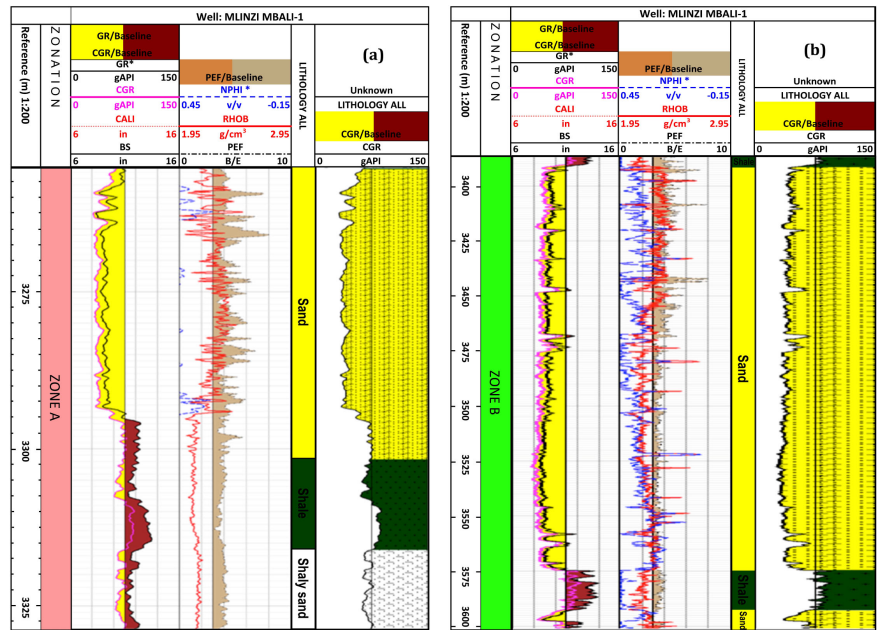


Figure 3. Log curves indicating reservoir for (a) Zone A and (b) Zone B.

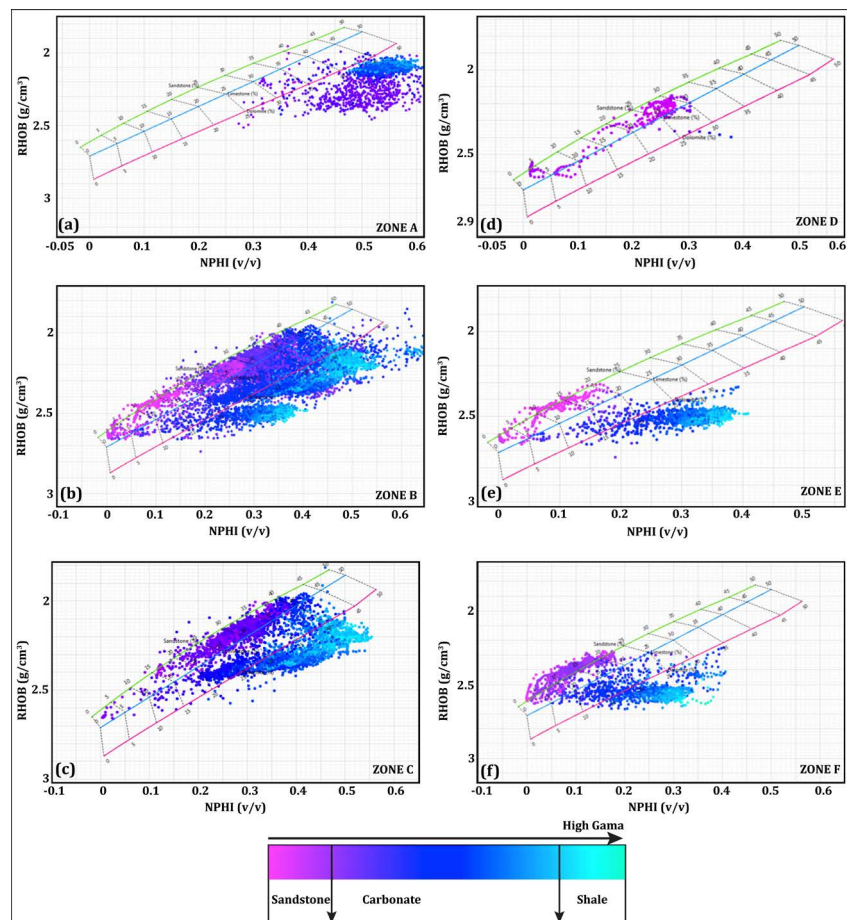


Figure 4. Neutron-density crossplots (a)-(f) for Zones A-F respectively, indicating the types of lithology. Gamma scale bar indicates the variations of color based on the relative intensity of gamma ray value.

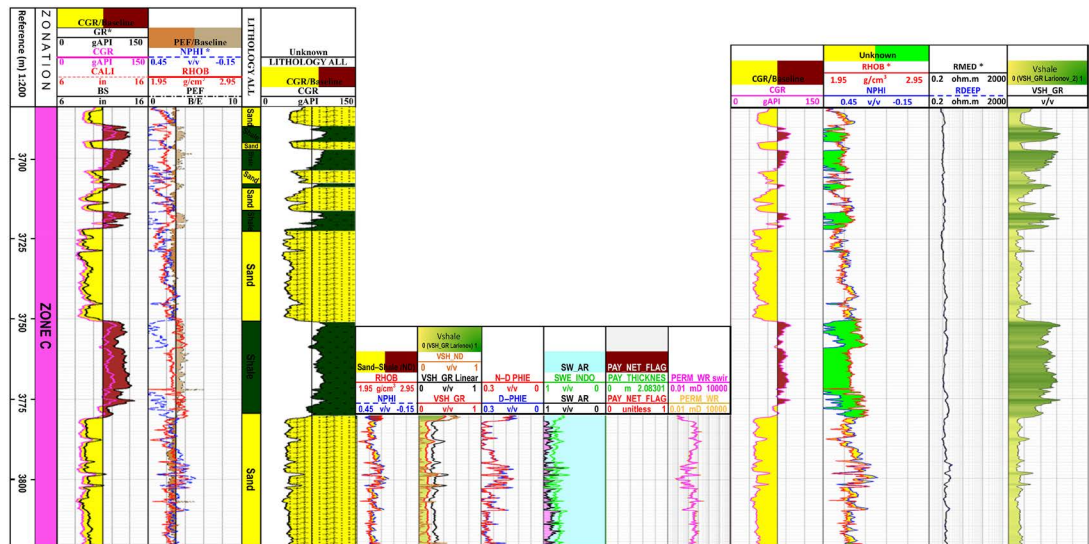


Figure 5. Log curves showing the types of lithology, neutron-density crossover and the computed petrophysical results for Zone C.

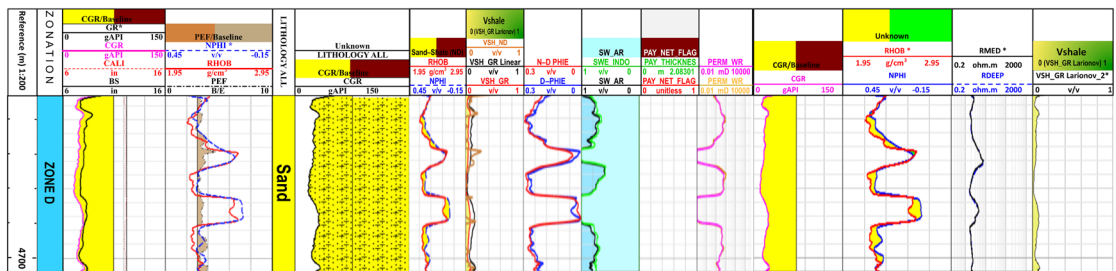


Figure 6. Log curves showing the types of lithology, neutron-density crossover and the computed petrophysical results for Zone D.

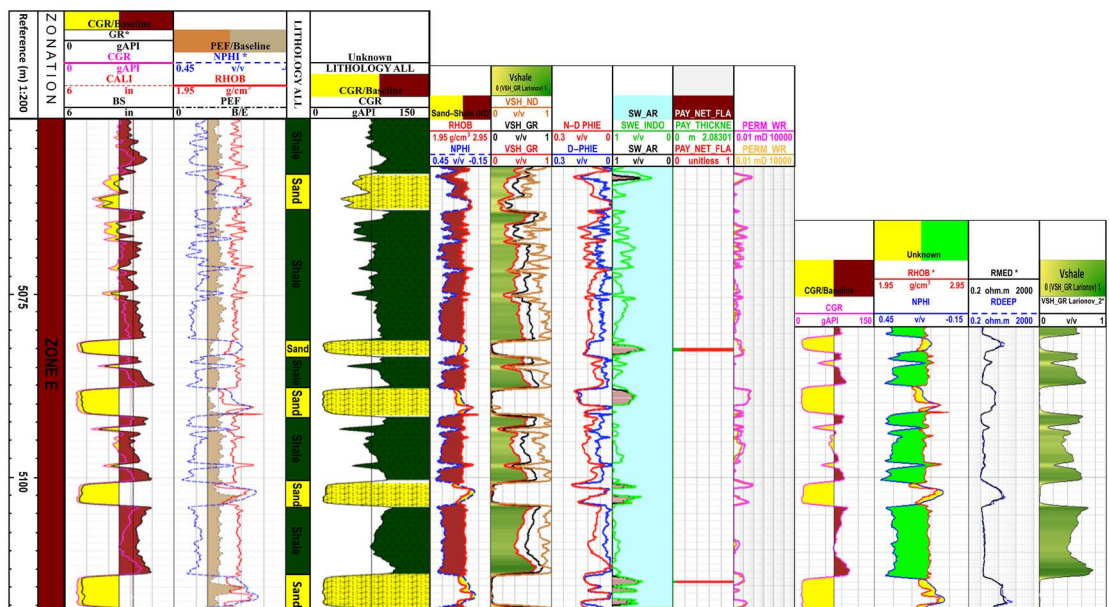


Figure 7. Log curves showing the types of lithology, neutron-density crossover and the computed petrophysical results for Zone E.

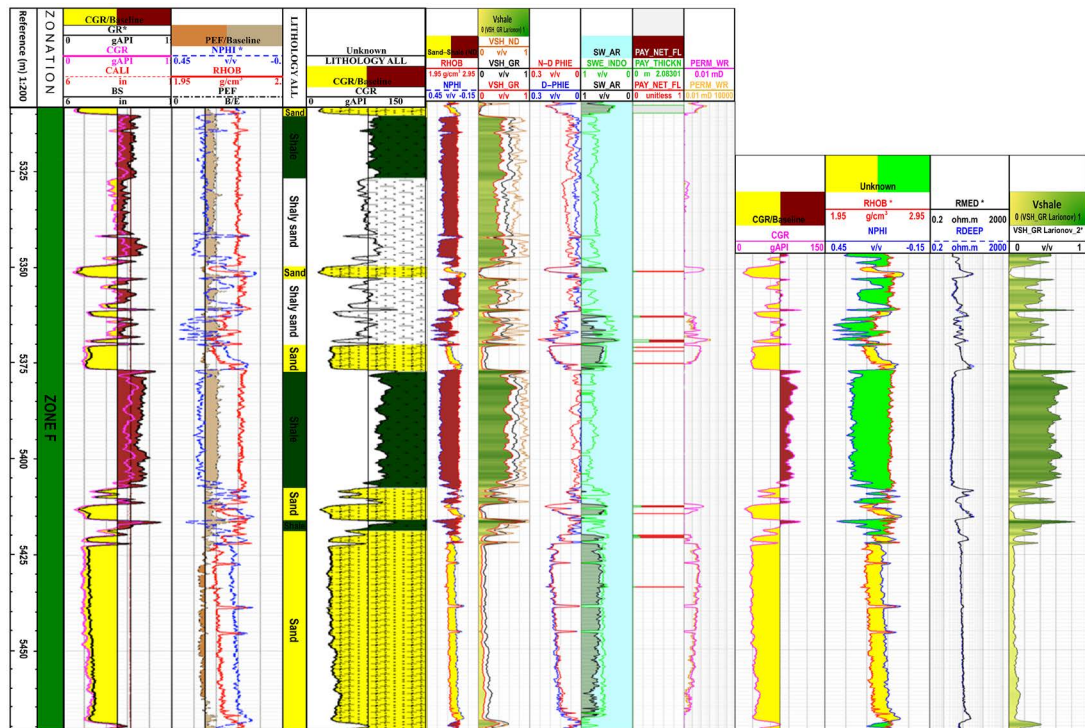


Figure 8. Log curves showing the types of lithology, neutron-density crossover and the computed petrophysical results for Zone F.

which occur in small intervals and are discontinuous. The crossovers between neutron-density logs are observed in some intervals and are marked by yellow colour and presented in respective log curves in **Figures 5-8** for zones C, D, E and F respectively. None of the four selected zones show signs of liquid hydrocarbon at the Mchungwa well.

4.2. Quantitative Interpretation

Average petrophysical values for each reservoir are shown in **Table 3** and results for computed petrophysical parameters for zones C, D, E and F are presented in **Figures 5-8** respectively. Reservoir sand qualities vary widely where the net reservoirs zones and net pay thicknesses range from 4.45 m to 59.08 m, and 0 to 2 m respectively. The shale volume for Zone C is observed to be higher (ranging from 0.10 to 0.17 (10% to 17%)) than in zones D, E, and F, which have very low values of 0.05, 0.08, and 0.08 respectively. Both average total and effective porosities range from 12% to 26% and 7% to 22% respectively (**Table 4**), and average water saturation for reservoirs zone ranges from 60.7% to 97.6% while water saturation in pay zone for zones E and F are 48.3% and 40.7% respectively. Permeability results range from 0.13 mD to approximately 6 mD. Hydrocarbons saturation results show that over 50% in reservoirs is water and the hydrocarbon (gas) is less than 20% in zones C and D and hydrocarbon saturation in pay zones E and F are 51.7% and 59.3% respectively. Generally porosity, water saturation and permeability decrease with depth.

Table 3. Summary of petrophysical parameters evaluated from Mchungwa well.

Zones	Flag name	Top (m)	Bottom (m)	Gross (m)	Net (m)	N/G	Vsh (v/v)	Porosity (%)	Sw-AR (%)	Sw-INDO (%)	SH (%)	Swir	K (mD)
C	Pay	3683.10	3911.80	228.70	42.20	0.19	0.15	23	97.6	82.4	2.4	91	2.99
	Res	3683.10	3911.80	228.70	0.00	0.00							
D	Pay	4688.07	4701.00	12.93	4.45	0.35	0.05	19	82.1	76.8	18	80	2.66
	Res	4688.07	4701.00	12.93	0.00	0.00							
E	Pay	5044.90	5118.05	73.15	12.90	0.18	0.08	10	80.8	76.7	19	78	0.03
	Res	5044.90	5118.05	73.15	0.21	0.00	0.01	12	48.3	48.0	52		
F	Pay	5305.00	5477.60	172.60	59.08	0.34	0.08	9	60.7	55.6	39	55	0.13
	Res	5305.00	5477.60	172.60	2.08	0.02	0.06	11	40.7	41.4	59		

Table 4. Porosity results for Zones C, D, E and F.

Zones	Av N-D PHIE (%)	Av N-D PHIT (%)	Av D PHIE (%)	Av D PHIT (%)
C	23	26	22	25
D	19	20	17	19
E	10	14	6	9
F	9	12	7	10

5. Discussion

5.1. Qualitative Interpretation

5.1.1. Lithology

The petrophysical analysis of the Mchungwa well qualitatively identified four zones of lithology, which were then used to delineate the free shale lithology and shale formation. The dominant lithology encountered were shale (probably claystone and siltstone) and free shale lithology interpreted by low gamma value. The dominant free shale lithology is sandstone, which is interbedded with shale, in some intervals, while other intervals the PEF value indicates the presence of carbonate lithology (limestone and dolomite), which probably occurs as cement in sandstone. However, core data and core cuttings are needed for final verification but these were not included in the study. Therefore, to minimize uncertainties in interpretation, lithology type has been narrowed down to sand and shale lithology.

5.1.2. Reservoir and Hydrocarbon Zones

The reservoir zones were identified qualitatively by marking the clean sand zones, which were designated as zones A, B, C, D, E and F. Based on high resistivity value and neutron-density crossovers observation, four Zones (*i.e.*, C, D, E and F) were marked as hydrocarbon zones while zones A and B were interpreted as non-hydrocarbon zones because of absence of neutron-density crossovers and low resistivity values. In the previous petrophysical interpretation by Ophir,

Dominion Tanzania Ltd (2014) (unpublished report) four reservoirs were identified and named as Maastrichtian (3760.0 m - 3912 m), Core Mlinzi channel (4605 m - 4701 m), Mlinzi deep (5341 m - 5496 m) and Mid to Late Jurassic (5496 m - 5782 m). Of the four reservoirs identified by Ophir, Dominion Tanzania Ltd (2014), the first three were also identified (with their respective depth ranges in brackets) in this study and are named here as Zones C (3683.1 m - 3911.8 m), D (4688.1 m - 4701 m) and F (5305 m - 5477.6 m) respectively. There is difference in the top and base of the reservoirs identified in this study as compared to those of previous study. Zone E identified in this study was not marked and interpreted by Ophir, Dominion Tanzania Ltd (2014) and therefore this is a new zone identified by this study. The Mid to Late Jurassic reservoir recognized by Ophir, Dominion Tanzania Ltd (2014) is not noted as a reservoir in this study because this interval or zone was identified as shale with little sandstone zone at Mchungwa.

5.2. Quantitative Interpretation

5.2.1. Net Thickness and Hydrocarbon Potentiality

The four selected reservoirs were analyzed quantitatively to estimate the values of shale volume, porosity, and fluid content through the use of empirical equations described in the methodology section. The net thicknesses of these four reservoirs after applying shale volume and porosity cutoff value were determined and indicated that sandstone reservoir in Zone F is thicker than other three zones (**Table 3**). However, after applying the water saturation cutoff value of 50% in order to define the net pay thickness (the economic zone with high hydrocarbon amount) Zones C and D gave zero net pay thickness. This indicates that Zones C and D contain more than 50% water implying that they are non-economical hydrocarbon zones. These zones are also characterized by thin/small crossovers and relative low resistivity values, which could be interpreted as the presence of an extremely low amount of gas but these crossovers could also be attributed to other factors. In some cases crossovers can arise from lithological differences as scaling effect where it could be sandstone recorded on limestone scale, or limestone recorded on dolomite scale [23].

The net pay thickness in Zones E and F are 0.2 m and 2.08 m respectively. In these small intervals water saturation is 48.3% in Zone E and 40.7% in Zone F. This indicates that the hydrocarbon saturation in Zones E and F are 51.7% and 59.3% respectively. However, these zones have not been considered as potential production targets because of the thin thickness of the pay zones. Compared to the previous study by Ophir, Dominion Ltd (2014) it shows that all four selected reservoirs have zero pay net thickness and 100% water saturation. The minimal variation of the results in this study and the previous study is probably due to difference in cut-off parameters used or the approaches that were used in calculations. Generally, hydrocarbon production potential at Mchungwa well is extremely low that could be attributed to natural geologic variability.

5.2.2. Shale Volume, Porosity and Permeability

Shale volume analysis results (see **Table 3**) show that the reservoir zones can be classified as clean sand and shaly sand. Zone C in this study was classified as shaly sand with average shale volume of 0.15 v/v, while Zones D, E, and F were classified as clean sand with average shale volume of 0.05 v/v, 0.08 v/v and 0.08 v/v respectively. The effective porosity results of the delineated reservoir units vary widely ranging from 7% to 23% indicating that reservoirs quality is in the range of good to poor. Zones C, D and E are classified as good quality reservoirs while Zone F is classified as poor quality reservoir with porosity less than 10%. In general permeability results show that the rocks at Mchungwa well have low permeability suggesting that the flow of fluid is very poor and hence have poor production capacity. Both porosity and permeability decrease with depth, which is probably due to increase of compaction and cementation with depth, associated with subsidence in the basin.

5.3. Geological Implication on the Petrophysical Properties

Petrophysical results at Mchungwa well is strongly affected by the regional and local geology of the area, so these results could be used to visualize and give broad context for the reservoirs' quality in the nearby area. High shale volume in Zone C (Maastrichtian Sandstone) was deposited during Late Cretaceous major transgression period where marine argillaceous sediments were frequently deposited with turbidity sandstones than sandstones deposited in Early Cretaceous (Zones D, E, and F). Sandstone reservoirs in Zone C (Maastrichtian), Zone D (Albian) and Zone E (Upper Hauterivian to Barremian) have good porosity. However, a regional decrease in porosity value could be due to cementation caused by dewatering of the thick sequence of Hauterivian to Campanian hemi-pelagic claystone, which surround porous Albian sand and underlie the Maastrichtian sand. Cementation by dewatering of the hemi pelagic claystone could also be the major reason for low permeability in the well. High water saturation in the identified sandstone reservoir sections and low hydrocarbon concentrations suggest the presence of non-commercial volumes of either migrant gas or gas generated from the interbedded claystone sediments which are dominant observed in the well.

6. Conclusion

Qualitative and quantitative interpretations of petrophysical properties of the reservoirs from well logs analysis in this study were successfully done. Results show that the delineated reservoir units of Mchungwa well have porosity ranging from poor to good of which Zones C, D and E have good porosity reservoir quality and Zone F has poor porosity reservoir quality. The reservoir sections with good porosity reservoir quality indicate that the grain sizes of these three reservoirs are uniform and coarse with low cementation. The permeability results obtained from well log in this study are negligible. Hence, the sandstones

are classified as impermeable. Despite of good porosity, the quality of the reservoirs sections can be categorized as poor due to poor permeability. The quality of the reservoirs was probably affected by dewatering of hemipelagic claystone. It is also observed that, the quality of the reservoirs decreases with depth, most likely due to the diagenesis and compaction associated with depth of burial of the older sediments during deposition. Generally, the field under study does not have good prospect for exploration and production because of the high level of water saturation and consequently low hydrocarbon saturations. However, the petrophysical information obtained from Mchungwa well provides vital information on regional geologic variability to enable further exploration in Northern offshore blocks in Tanzania.

Acknowledgements

The authors are grateful to the BG Group for funding this research as part of MSc. study under K2K project. We thank Tanzania Petroleum Development Company (TPDC) for providing the data used in this study. We extend sincere appreciation to many individuals from the University of Dar es Salaam and TPDC for their assistance in completion of this work. We also thank anonymous reviewers for helpful comments.

References

- [1] Kent, P.E., Hunt, J.A. and Johnstone, D.W. (1971) Geology and Geophysics of Coastal Sedimentary Basins of Tanzania. Institute of Geological Sciences, Geophysical Paper, London, Vol. 6, 1-101.
- [2] Zongying, Z., Ye T., Shujun, L. and Wenlong, D. (2013) Hydrocarbon Potential in the Key Basins in the East Coast of Africa. *Elsevier Science*, **40**, 582-591.
- [3] Rabinowitz, P.D., Coffin, M.F. and Falvey, D. (1983) The Separation of Madagascar and Africa. *Science*, **220**, 67-69. <https://doi.org/10.1126/science.220.4592.67>
- [4] Salman, G. and Abdula, I. (1995) Development of the Mozambique and Ruvuma Sedimentary Basins Offshore Mozambique. *Sedimentary Geology*, **96**, 7-41. [https://doi.org/10.1016/0037-0738\(95\)00125-R](https://doi.org/10.1016/0037-0738(95)00125-R)
- [5] Danforth, A., Granath, J., Horn, B. and Komba, K. (2012) Hydrocarbon Potential of the Deep Offshore Tanzania Basin in Context of East Africa's Transform Margin. East Africa: Petroleum Province of the 21st Century. London, 24-26 October 2012, 32-33.
- [6] Zhixin, W., Zhaoming, W., Chengpeng, S., Zhengjun, H. and Xiaobing, L. (2015) Structural Architecture Differences and Petroleum Exploration of Passive Continental Margin Basins in East Africa. *Petroleum Exploration and Development*, **42**, 733-744. [https://doi.org/10.1016/S1876-3804\(15\)30070-7](https://doi.org/10.1016/S1876-3804(15)30070-7)
- [7] Kajato, H. (1982) Gas Strike Spurs Search for Oil in Tanzania. *Oil Gas Journal*, **123**, 123-131.
- [8] Kreuser, T., Wopfner, H., Kaaya, C.Z., Markwort, S., Semkiwa, P.M. and Aslandis, P. (1990) Depositional Evolution of Permo-Triassic Karoo Basins in Tanzania with Reference to Their Economic Potential 1990. *Journal of African Earth Sciences (and the Middle East)*, **10**, 151-167. [https://doi.org/10.1016/0899-5362\(90\)90052-G](https://doi.org/10.1016/0899-5362(90)90052-G)
- [9] Mpanda, S. (1997) Geological Development of the East African Coastal Basin of

- Tanzania. *Stockholm Contributions in Geology*, **45**, 11-108.
- [10] Bourget, J., Zaragosi, S., Garlan, T., Gabelotaud, I., Guyomard, P., Dennielou, B. and Schneider, J. (2008) Discovery of a Giant Deep-Sea Valley in the Indian Ocean, off Eastern Africa: The Tanzania Channel. *Marine Geology*, **255**, 179-185.
<https://doi.org/10.1016/j.margeo.2008.09.002>
- [11] Kapilima, S. (2003) Tectonic and Sedimentary Evolution of the Coastal Basin of Tanzania during the Mesozoic Times. *Tanzania Journal of Sciences*, **29**, 1-16.
- [12] Teixeira, L., Martinez, V. and Chrispin, S. (2009) Tanzania Ultra-Deepwater Exploration. *Search and Discovery*, 1-9.
- [13] Scrutton, R.A. (1997) Davie Fracture Zone and the Movement of Madagascar. *Earth and Planetary Science Letters*, **39**, 84-88.
[https://doi.org/10.1016/0012-821X\(78\)90143-7](https://doi.org/10.1016/0012-821X(78)90143-7)
- [14] Bassiouni, Z. (1994) Theory, Measurement and Interpretation of Well Logs. Textbook Series, Society of Petroleum Engineers (SPE), Vol. 4.
- [15] Ellis D.V. and Singer, J.M. (2008) Well Logging for Earth Scientists. 2nd Edition, Springer, Berlin.
- [16] Asquith, G.B. and Gibson, C.R. (1982) Basic Well Log Analysis for Geologists. The American Association of Petroleum Geologists (AAPG), Tulsa.
- [17] Serra, O. (1986) Fundamentals of Well-Log Interpretation. 2. The Interpretation of Logging Data, Developments in Petroleum Science. Developments in Petroleum Science, 15B, Elsevier, Amsterdam.
- [18] Larionov, V. (1969) Radiometry of Boreholes. NEDRA, Moscow.
- [19] Archie, G.E. (1942) The Electrical Resistivity Log as an Aid in Determining Some Reservoir Characteristics. *Transactions of AIME*, **146**, 54-62.
<https://doi.org/10.2118/942054-G>
- [20] Poupon, A. and Leveaux, J. (1971) Evaluation of Water Saturation in Shaly Formations. *The Log Analyst*, **12**, 1-2.
- [21] Timur, A. (1968) An Investigation of Permeability, Porosity and Residual Water Saturation Relationships for Sandstone Reservoirs. *The Log Analyst*, **9**, 3-5.
- [22] Crain, E.R. (1986) The Log Analysis Hand Book. Penn-Well, Publ. Co., Tulsa.
- [23] Crain, E.R. (2016) Visual Analysis Rule for Water Saturation, Petrophysical Hand-out. <https://www.spec2000.net/>